Journal of Optoelectronics and Advanced Materials Vol. 5, No. 4, December 2003, p. 1003 - 1009

*Section 5c SUPERCONDUCTING MATERIALS*
*Invited paper*

# ENHANCED SUPERCONDUCTING PROPERTIES IN LI-DOPED BPSCCO HIGH-$T_c$ CERAMICS

G. Aldica*, J. R. Groza[a], K. Endo[b], H. Kito[b], V. Mihalache

National Institute R&D for Materials Physics, P. O. Box MG-7, RO-76900, Bucharest, Romania
[a]Department of Chemical Engineering and Materials Science, University of California, Davis, California 95616-5294, USA
[b]NeRI of National Institute for Advanced Industrial Science and Technology, AIST Tsukuba Central 2, 1-1-1 Umezono, 305-8568, Tsukuba, Ibaraki, Japan

Superconductors are currently used only in low scale applications where other materials cannot compete with their unique properties. High-Tc superconductors are highly processing sensitive and, therefore, prohibitively expensive at this time. A new technique, Field-Assisted-Sintering Technique (FAST), is proposed for superconductors to shorten the processing time. It combines the use of an external electrical field with pressure application at a high heating rate, thus making the processing time less than 15 min. We have applied this method to the decomposition of the precursor powders with different starting cations in Bi-Pb-Sr(Ba)-Ca-Cu-O system. In some compositions LiI has been added. Enhanced formation of $Bi_2Sr_2Ca_2Cu_3O_x$ phase in Ba-substituted BPSCCO ceramics was observed in FAST-treated and post-annealed samples. All compositions have high density depending on starting composition.

(Received July 14, 2003; accepted August 21, 2003)

*Keywords*: Superconductivity, Bi-Pb-Sr(Ba)-Ca-Cu-O system, Field Assisted Sintering Technique (FAST), AC magnetic susceptibility, LiI addition.

## 1. Introduction

Bi-based materials exhibit a high value of anisotropy factor, and a weak flux-pinning effect at 77.3 K and above, which result in serious limitations of their practical applications. However, considering the high critical temperature of $Bi_2Sr_2Ca_2Cu_3O_{10+x}$ (denoted by 2223) phase, engineering the doping with various atoms may increase of the critical current density. The relatively high solubility limit of Li in $Bi_2Sr_2CaCu_2O_{8+\delta}$ (denoted by 2212) single crystal (Li/(Li+Cu) = 13 %) allows for a systematic study of the influence of the doping level on the synthesis conditions and supenconducting parameters of high-$T_c$ phases in the Bi-Sr-Ca-Cu-O system [1-3].

Our previous studies of LiF [4,5]- and LiI [6] - doped BPSCCO systems revealed that a small quantity of lithium compound helps the formation of the high-$T_c$ superconducting phase (2223), whereas at a higher doping level it induces the formation of the low-$T_c$ superconducting phase (2212), and thus reduces the content of 2223-phase. Therefore, there is a critical amount of LiI to maximise the volume fraction of 2223-phase, critical temperature, inter-grain critical current density and intra-granular critical current density. Also a split of the peak in out-of-phase susceptibility corresponding to the dissipation in the grains was observed.

On the other hand, high-$T_c$ superconductors are very sensitive to processing and, prohibitively expensive at this time. By the application of new consolidation method, Field-Assisted-Sintering-Technique (FAST) to sintering of undoped and Li-doped powders, shorter sintering times and dense

* Corresponding author: aldica@alpha1.infim.ro

superconducting ceramics have been obtained [7]. FAST combines the use of an external electrical field with pressure application at a high rate and short processing times [8]. Low pressure (below 100 MPa), but high pulsed current through powder (nearly 1 kA) are used. The process involves fewer steps in powder densification since no prior cold pressing or additives are necessary.

In this work, we studied the influence of LiI during FAST application to powders with different compositions to enhance the formation of the 2223-phase.

## 2. Experimental

High-purity $Bi_2O_3$, PbO, $SrCO_3$, $CaCO_3$ and CuO powders were mixed in the ratio Bi:Pb:Sr:Ca:Cu = 1.7:0.4:1.5:2.5:3.6 (type A) and Bi:Pb:Sr:Ba:Ca:Cu = 1.8:0.4:1.8:0.2:2:3 (type B), then thoroughly ground in an agate mill and calcined in an alumina crucible at 800-820 °C for 20 h in air. After re-grinding the compound A, a quantity of powder (exhibiting particles with diameter less than 40 μm) was doped with $(LiI)_{0.1}$, well mixed in an agate mortar and pressed in 12×9×3 $mm^3$ pellets at 0.75 GPa. The compound B was only re-ground and pelletized. The sintering thermal treatment of the pellets was performed in air, for 300 h, at 837±2°C. Both type of pellets were re-ground. Then, the specimen of powder B was mixed with $(LiI)_{0.13}$.

Each of these powders were loaded into the punch and die carbon unit (20 mm in diameter) of the FAST machine. FAST processing was performed in vacuum **(**10 Pa**)**, using "Dr. Sinter Spark Plasma Sintering System" (Sumitomo Coal Mining Co, Japan). The temperature and time of FAST processing for each sample are shown in Table 1. The external die temperature was measured using a pyrometer and the inside temperature was monitored by a T-type thermocouple. No significant temperature difference was detected. An uniaxial pressure of 17.5 MPa applied throughout the whole sintering cycle was used for all samples (denoted by AF and BF). The pulsed power current cycle was in 12 ms on and 2 ms off duration. Shrinkage and shrinkage rate during reactive-consolidation process were plotted "in situ" by computers attached to the FAST machine. After sintering, a heat treatment (HT) was applied at 849°C for 70 hrs, in air (samples noted by AFT and BFT).

In fact, we have chosen these two type of compounds for our studies because of the great difference in Bi-2223 phase concentration and of the much lower inter-grain (transport) critical current density of samples in compound A. Since the properties of superconducting phases of BPSCCO system depend strongly on the sintering conditions, we treated all the pellets in a batch together, in the same furnace.

The density of the pellets was determined from geometry and weight measurements. X-ray diffraction (XRD) patterns on powders and FAST-pellets (ground and not ground) were obtained with a Scintag Automated Diffractometer fitted with a solid-state counter and $CuK_{\alpha 1}$ radiation ($\lambda_{K\alpha 1}$=1.54059 Å) in the range $2\theta$ = 10 to 80º. The microstructure and micro-composition of the samples were analysed using a JSM-6301F scanning electron microscope (SEM) equipped with an EDS system. The electrical resistivity was measured by the standard four-probe method, using silver paint for electrical contacts. The Seebeck coefficient was measured at room temperature, using the warm point method and a platinum reference. The transport critical-current density $J_{ct}$ was determined at $T$ = 77.3 K in zero applied magnetic field, using the criterion of 1 μV/cm. The AC susceptibility measurements were performed using the lock-in amplification technique, at a fixed frequency of 5.5 kHz, temperatures down to 77.3 K, and AC field amplitudes $H_{ac}$ between 5 and 100 A/m. The superimposed *DC* magnetic field $H_{dc}$ was between 0 and 14 kA/m. The magnetic signal was measured on samples cooled from 150 to 77 K with cooling rates less than 1 K $min^{-1}$ and was normalised to the weight of the samples. The *DC* magnetisation measurements were performed at 77.3 K, up to a field value of 150 kA/m, using an integrator magnetometer (Thor Cryogenics 9020II).

## 3. Results and discussion

FAST pellets have bulk densities between 5.6 and 5.9 g $cm^{-3}$ (Table 1). These values are 88-91% of the theoretical densities of the 2212- and 2223-phases, if we consider that the whole

sample consists of both phases. In a standard process, the pellets (~ 60 min treated) have bulk densities between 4 and 4.5 g $cm^{-3}$.

Table 1. Samples, FAST regime, and bulk density of the pellets after FAST.

| Sample | FAST process | | | |
|---|---|---|---|---|
| | Heating ramp [°C] / [min] | Holding temperature and time [°C] / [min] | Peak temperatures in shrinkage rate [°C] | Bulk density [$g/cm^3$] |
| AF | 20-700 / 9; 700-750 / 1 | 750 / 4 | 437; 480; 590; 625 | 5.95±0.01 |
| BF | 20-700 / 9; 700-750 / 1 | 750 / 4 | 615; 650 | 5.62±0.01 |

The shrinkage displacement and shrinkage rate curves measured in situ during FAST have different shapes. Peaks in the shrinkage rate curves (i.e., the maximum shrinkage rate) occurs at different temperatures, depending on the sample (Table 1). The intensity of the peak is also changing. The peak temperatures for shrinkage (densification) rates strongly depend on starting stoichiometry. The lower peaks occur with more Ca and Cu in the nominal composition of samples. When temperature is held constant the shrinkage displacement and shrinkage rate do not vary indicating an apparent equilibrium temperature for densification of the material.

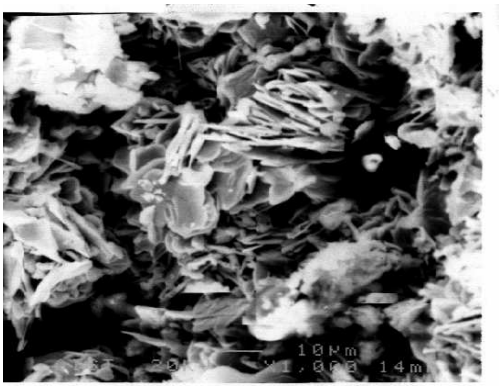

Fig. 1a SEM image for the pellet of type A before FAST process (x1000).

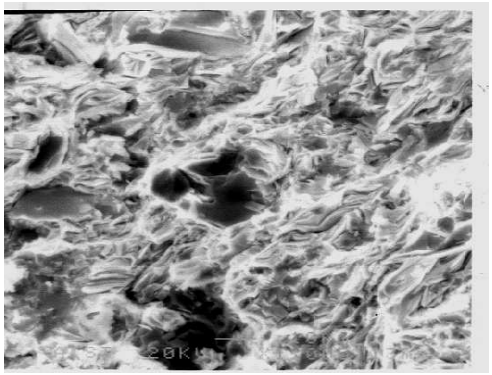

Fig. 1b SEM image for the pellet of type A after FAST process (x1000).

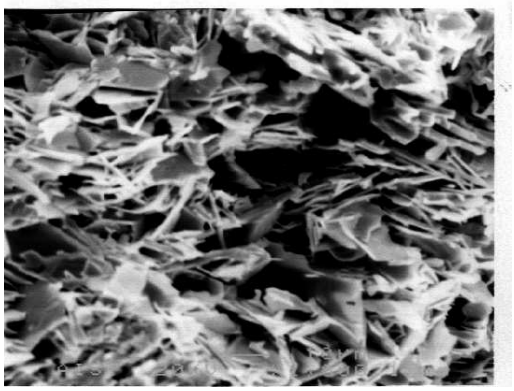

Fig. 1c. SEM image for the pellet of type B before FAST process (x1000).

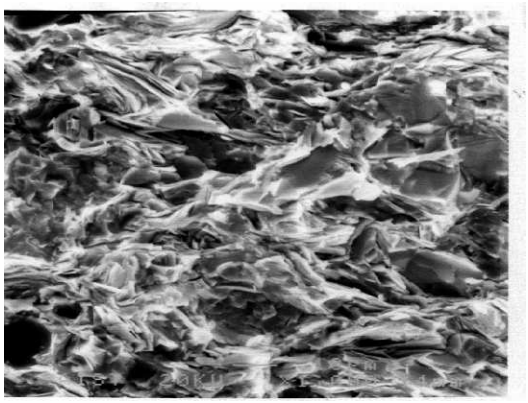

Fig. 1d. SEM image for the pellet of type B after FAST process (x1000).

SEM images of fresh fracture surfaces of as-synthesised and FAST pellets are presented in Fig. 1. As –synthesised samples of both types exhibit a dispersed, thin plate-like crystallites. After

FAST process, relatively fully packed and non-porous grains with a plate-like morphology specific to superconducting 2212/2223-phases can be observed, while the grain dimension remains practically unchanged (7-15 μm). Also, by LiI doping, one observes an increase of the melted material during the sintering process, leading to grain rounding. From EDS data, the sample AF contains 2212 and 2223-phases, which are Bi rich and Ca poor. All BF samples are compositions poor in Sr and Ca. The plate-like crystallites contain a Bi enriched 2223-phase. In all EDS observations on B and BF samples, a lower Ba content than the nominal value was detected.

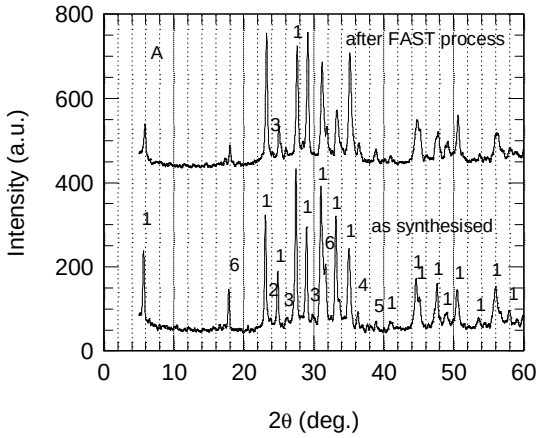


Fig. 2a. XRD patterns for sample of type A 1-2212; 2-2223: 3-2201; 4-$(Ca,Sr)_2CuO_3$; 5-CuO; 6-$(Ca,Sr)_2PbO_4$;

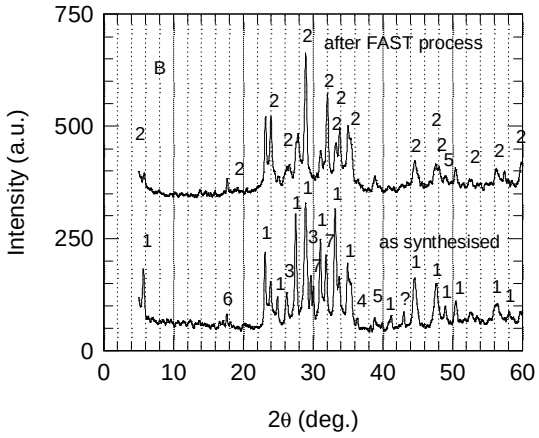


Fig. 2b. XRD patterns for sample of type B 1-2212; 2-2223: 3-2201; 4-$(Ca,Sr)_2CuO_3$; 5-CuO; 6-$(Ca,Sr)_2PbO_4$; 7-$(Sr,Ca)CuO_2$

The volume fraction $f$ of the high-temperature superconducting 2223-phase was estimated from *XRD* as:

$$f = \frac{A(0010)_{2223}}{A(0010)_{2223} + A(008)_{2212}} * 100\%, \quad (1)$$

where $A(0010)_{2223}$ and $A(008)_{2212}$ represent the peak area for the reflections $(0010)_{2223}$ and $(008)_{2212}$ respectively. There is a maximum in the 2223 content (50 % for sample B after FAST), as shown in Fig. 2. Comparison of XRD patterns obtained on type A and B pellets before and after FAST process has indicated a significant [00*l*] texture for 2212-phase (about 0.65).

The temperature dependence of the electrical reduced resistance $R/R^{300K}$ is illustrated in Fig. 3. Samples of type B exhibit less semiconducting and more metallic behaviour, whereas samples of type A show only metallic behaviour. After 70h HT, both types of samples show the characteristics of the superconducting 2223-phase.

The Seebeck coefficient, α, is, in a first approximation, a measure of the deviation from metallic behaviour of the sample in normal state. As can be seen in Table 2, α has negative and positive values, at some μV/K level. This is mainly due to the contribution of doping elements to α by the selective substitution of cations and oxygen. According to Refs. [9] $\alpha$ is small when the carrier concentration is high.

Table 2. Seebeck coefficient and transport critical current density for all samples.

| Sample | A | $A(O_2)$ | AF | $AF(O_2)$ | AFT | B | $B(O_2)$ | BF | $BF(O_2)$ | BFT |
|---|---|---|---|---|---|---|---|---|---|---|
| α (μV) | 3.8 | -1.2 | 1.3 | -3.5 | 1.4 | 2.8 | 0.3 | 6.0 | -4.5 | 7 |
| $J_{ct}$ ($A/cm^2$) | 0.001 | NA | 0 | NA | 150 | 0.7 | NA | 0 | NA | 85 |

Note: Samples A, AF, B and BF were treated in $O_2$ atmosphere at 300 °C for 2 h.

In-phase and out of-phase susceptibility measurements in *AC* field with $H_{ac}$ = 5 A/m without a superimposed DC field are presented in Fig. 4 and 5 for samples A, AF and B, BF, respectively.

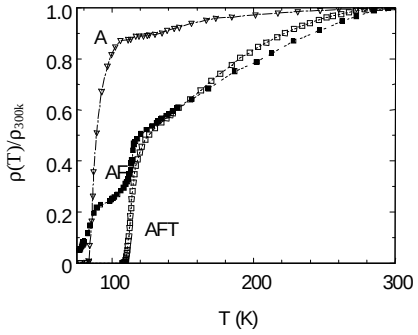


Fig. 3a. Temperature variation of the reduced resistivity for samples of the type A.

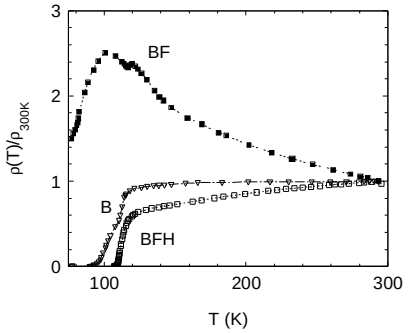


Fig. 3b. Temperature variation of the reduced resistivity for samples of the type B.

The absolute value of $\chi$' signal for sample A in Fig. 4 corresponds to the diamagnetic signal in 2223-grains (the inter-granular coupling is weak and the respective signal is shifted under 77.3 K) and denotes a small quantity of 2223-phase. It can be seen that the majority of the 2223-phase of sample A is a "110 K"-phase whereas the majority of 2223-phase of sample AF is a "100 K"-phase. The examination of these results against those measured at R(T) measurements shows that the majority of weak-links in sample A are of poor quality; the 2223-phase amount (which leads to the "110 K" step in $\chi$') of the same sample is insufficient for the percolation at 110 K. The small amount of 2223-phase in the AF sample (the 2223-phase signal is not even visible in $\chi$') has a quite high signal in R(T) because the enhancement of the coupling between 2223-grains occurs, despite the fact that there is no percolation in this case. *Therefore, FAST can lead to the enhancement of coupling between the 2223-grains*. The orientation of the grains may explain this feature.

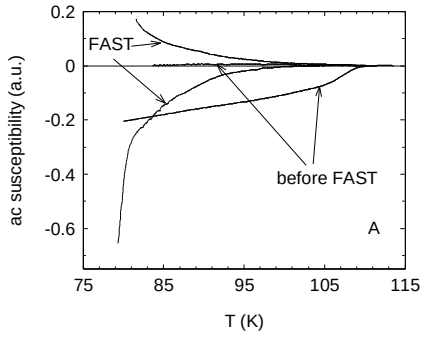


Fig. 4. AC susceptibility vs. temperature in $H_{ac}$ = 5 A/m for samples of the type A.

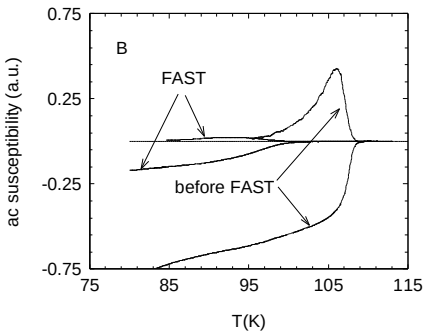


Fig. 5. AC susceptibility vs. temperature in $H_{ac}$ = 5 A/m for samples of the type B.

The main dropping in R(T) of sample A corresponds to poor links between 2223-grains than to the 2212-phase. The drop at 86-87 K in $\chi$' for sample A is less than for R(T) curve. In contrast, such a dropping is seen in both $\chi$' (T) and R (T) curves at 80-81 K in the AF sample. These signals correspond to the Bi-2212 phase. Therefore FAST *process leads to a higher quality bonding, and to larger amount of Bi-2212 phase*. This may be also attributed to the presence of 0.1LiI because it is well known that Li enhances the Bi-2212 phase formation [10].

In the case of samples B and BF, doping with 0.13 LiI together with FAST process result in almost completely destroying the coupling between Bi-2223 grains (Fig 5). This is in good agreement with the results of R(T) measurements on these samples and denotes the presence of high quantity of

melting material. The comparison of Fig. 5 and Fig. 4 (sample B and sample A) may indicate that Ba substitution for Sr leads to more Bi-2223 phase formation and a better coupling between the grains.

We performed out-of-phase susceptibility measurement for all samples at a $H_{ac}$ = 100 A/m field with the different values of superimposed *DC* field. As a representative example could be the measurements data on sample AFT presented in Fig. 6. Fig. 7 shows the temperature dependence of the field for full penetration for all samples determined from the measurements at $H_{ac}$ =100 A/m with the different values of the superimposed *DC* field.

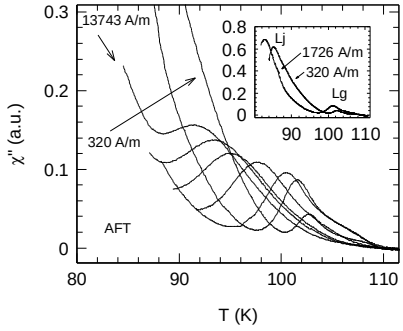


Fig. 6. $\chi$" vs. T in $H_{ac}$ = 100 A/m with the different values of *DC* field.

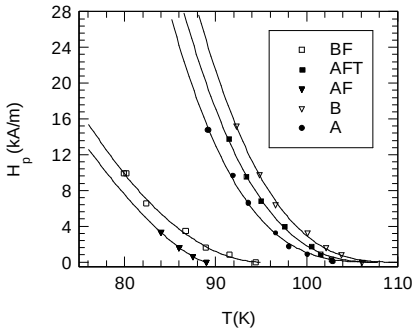


Fig. 7. Temperature dependence of the field for full penetration for all samples.

From the inset of Fig. 6 it can be seen that the inter-granular signal corresponding to the sample AFT measured at low values of DC fields is situated far above 77.3 K whereas for the sample A there is no inter-granular signal above 77.3 K. This result confirms that *FAST process following 70h heat treatment leads to a considerable enhancement of coupling between 2223-grains* and this is in good agreement with the results of R(T) measurements.

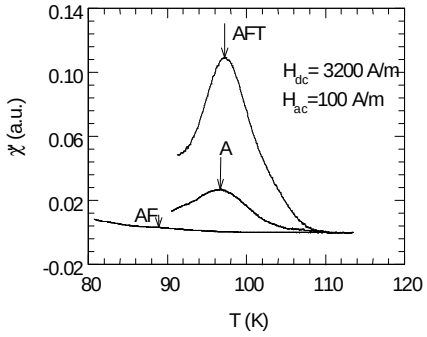


Fig. 8. $\chi$" vs. T in both applied magnetic fields for samples of the type A.

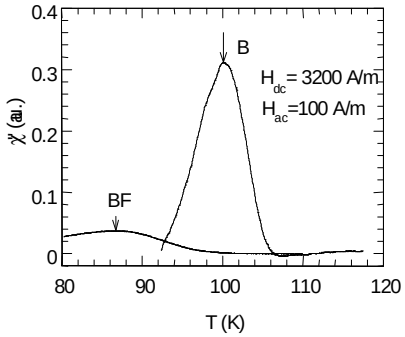


Fig. 9. $\chi$" vs. T in both applied magnetic fields for samples of the type B.

We can deduce from Fig. 7 that the FAST process strongly affects the strength of intra-granular (respectively $J_{cg}$) pinning in both A and B samples. Taking into account that the average size of grains after the FAST process did not change, one can say that the reason of this behaviour is the deterioration of grain boundaries. Thus the deterioration of grain boundaries can produce not only a decreasing of transport critical current density $J_{ct}$ (inter-granular critical current density), which is well known, but *can also produce a very strong impact on the intra-granular critical current density* $J_{cg}$. The better-oriented platelets in samples AF and BF unlike those of samples A and B do not influence our conclusions. But, on the contrary, these results support the conclusions because in the textured

bulk samples the curves $H_p(T)$ for the field applied in the direction of orientation is situated at higher values of $H_p$ than those for H applied perpendicular to the orientation.

Another important result shown by Fig. 7 is that after the *FAST process followed by a 70h heat treatment the strength of pinning increases comparatively to as-synthesised sample A.*

Fig. 8 presents the out-of-phase susceptibility curves for samples A, AF and AFT measured at $H_{ac}$ = 100A/m field and $H_{dc}$ equal to 3200 A/m. Also, it presents the similar curves for the B and BF samples. For the similar samples from the point of view of the grain size, type and the strength of the coupling, etc., the out-of phase signal can be used for the comparative estimation of the amount of 2223-phase. The only condition is to well separate the inter- and intra-grain peaks. From the comparison of the aria under the $\chi$" (T) peaks for samples A and AFT (Fig. 8) we can say that FAST process followed 70h heat treatment leads to an increasing up to 3-4 times of 2223-phase. *Therefore, this processing combination leads to an increase of the amount of 2223-phase.*

The distinct differences between the heights of peaks in A, AF (Fig. 8) and B, BF (Fig. 9) samples denote the higher volume fraction of 2223-phase in the B and BF bulk samples. This is due to the Ba substitution for Sr as much as to the 0.13 LiI addition in the FAST step.

A split of the peak corresponding to the losses in the 2223-grains especially in the samples A and AFT (see Fig. 6) was observed, similar to that observed in our previous work [6].

## 4. Conclusion

The role of LiI in the observed behaviour of FAST- and HT-processed samples is discussed in connection with the SEM and EDS analysis, X-ray diffraction data, resistivity, thermoelectric power and ac magnetic susceptibility measurements. Further studies on FAST processed BPSBCCO samples are expected to increase of 2223-phase and to enhance the superconducting parameters.

**Acknowledgements**

The Romanian Ministry of Education and Research supported this work under CERES Program. The FAST research has been supported by an NSF (USA) grant. A JSPS Fellowship for Research in Japan is gratefully acknowledged (G. Aldica).

## References

[1] T. Kawai, T. Horiuchi, K. Mitsui, K. Ogura, S. Takagi, S. Kawai, Physica C **161**, 561 (1989).
[2] T. Horiuchi, K. Kitahama, T. Kawai, Physica C **221**, 143 (1994).
[3] B. Gopalakrishna, M. Chandrasekhar, S. V. Suryanarayana, Cryst. Res. Tehnol. **30**, 411 (1995).
[4] V. Mihalache, G. Aldica, C. Giusca, L. Miu, J. of Superconductivity: Incorporating Novel Magnetism **14**, 575 (2001).
[5] V. Mihalache, G. Aldica, S. Popa and A. Crisan, Physica C **384**(4), 451 (2003).
[6] V. Mihalache, G. Aldica, Proceedings JINR-Romanian Workshop in Advanced Materials and their Characterization, ISBN 5-8481-0018-7, Editors V.V.Sikolenko, M.Balasoiu, Moscow, 51 (2003).
[7] P. Badica, G. Aldica, J.R. Groza, M. C. Bunescu, S. Mandache, Supercond. Sci. Technol. **15**, 32 (2002).
[8] J. R. Groza ASM Handbook, Vol **7** (Metals Park, OH: ASM), 583 (1998).
[9] R. F. Brebrick, in Defects in Solids, Vol. 2, Treatise on Solid State Chemistry, edited by N. B. Hannay (Plenum, New York, 1975) p. 357.
[10] E. D. Politova, I.V. Ol'chovik, G.M. Koleva, Yu.N. Venevtsev, Ferroelectrics **167,** 305 (1995).